Metals Materials And Processes, 2000, Vol. 12, No. 2 & 3, pp. 197 - 214.

BORON NITRIDE BASED CUTTING TOOLS

C.Divakar
High Pressure Laboratory, Materials Science Division,
National Aerospace Laboratories, Bangalore-560017, India.

(Received 10 January 2000)

Abstract : Diamond and cubic boron nitride (cBN) are two commonly used hard materials as cutting tools. Diamond the hardest substance known can cut all but ferrous materials because of its reaction with iron. cBN next to diamond in hardness can cut all ferrous materials because of its inertness. Diamond is available in nature, whereas boron nitride is man-made. Both these materials can be produced in the laboratory by the application of high pressures and temperatures. Wurtzite boron nitride (wBN) is a hard phase of boron nitride obtained by shock loading of hexagonal boron nitride (gBN). A composite of wBN-cBN is obtained by sintering of wBN at high pressures in the stablity region of cBN. The wBN-cBN compacts have an unique combination of high fracture toughness and hardness, which make the composite tool capable of machining under interrupted conditions. A four column 600-ton capacity press designed and fabricated for the sintering of ceramic materials at high pressures and temperatures has been used to prepare the wBN-cBN composite. The work done at the high pressure laboratory, Materials Science Division, National Aerospace Laboratories in the synthesis, sintering, fabrication and the evaluation of the wBN-cBN composite tools in the machining of various difficult-to-cut materials - hardened steels (HRC 40-63), high nickel cast iron (BHN 120-160) and Ti-6Al- 4V alloy (HV 310), and Al-SiC_p MMC (silicon carbide particulate reinforced aluminium based metal-matrix-composite) are presented in this paper.

Key words: boron nitride, cutting tool, synthesis, hardened steel, titanium alloy, MMCs, performance

1. INTRODUCTION

The demand for higher productivity and lower manufacturing costs has imposed a need for the development of cutting tools capable of operating at high cutting speeds. High machining speeds generate higher stresses and increase the temperature at the tool-workpiece interface and require better refractory tool materials. Cemented carbides, titanium carbide based cermets and alumina based ceramics are excellent cutting tool materials which show superior cutting performance in machining conventional steels and cast irons of normal hardness. However, in cutting hardened steels, chilled cast irons, super alloys and metal - matrix composites, these tools have a very short life and sometimes are unable to cut at all because of the cutting edge fracture. The difficult- to-cut materials are mostly shaped by grinding. A cutting tool expected to perform under severe machining condition should therefore have adequate fracture toughness, high hot hardness, thermal shock resistance, and must be chemically stable and inert at the operating temperatures.

The advancement in high-pressure technology has made it possible to develop a new generation of superhard materials based on diamond and cubic boron nitride[1-3]. In many situations, the final grinding operations of the difficult-to-cut materials can be replaced by turning operation with the tools made of these materials. The tools based on these materials have increased the cutting speeds by a factor of 100 over the turn of this century[4].

Detailed reviews are available on the properties of cubic boron nitride[5] and its processing for cutting tool applications[6-8]. The polycrystalline boron nitride (PCBN) tools have performed well over the years in the machining of hardened steels and creep resistant alloys. But the low fracture toughness of these tools imposes a serious limitation in their

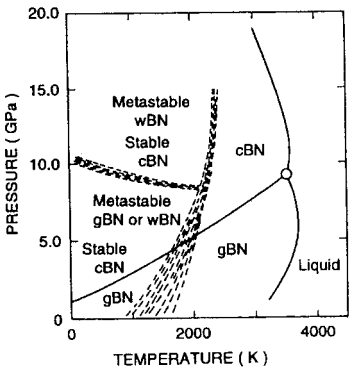

Fig.1. Phase diagram of boron nitride (Ref.16).

use under interrupted cutting conditions. Also the use of cBN tool requires high-speed, vibration-free rigid machines.

A composite tool based on the wurtzite and cubic modifications of boron nitride has been found to have better fracture toughness than that of PCBN tools, and perform well under interrupted cutting conditions[9-12]. They can also tolerate high level of vibration in the machines. In this paper, the synthesis of wBN, the high pressure-high temperature compaction of wBN powder and the performance of wBN-cBN tools in the machining of hardened steels, cast irons, titanium alloys and Al-SiC_p metal matrix composites are presented.

2. BORON NITRIDE

Boron nitride is known to exist in three different polymorphic forms : (i) hexagonal or graphitic (gBN), (ii) hexagonal wurtzitic (wBN) and (iii) the cubic zinc blende (cBN). Under ambient conditions, gBN is stable, and both wBN and cBN are the metastable phases[13,14].

The conversion of gBN to wBN takes place under the application of high pressures and temperatures. The gBN transforms to denser modifications at pressures over 10 GPa at and above room temperature without the aid of catalysts[15]. The phase diagram of boron nitride is shown is shown in Fig 1[16]. The dotted lines in the phase diagram delineate the gBN to metastable wBN or cBN, and metastable wBN or cBN to stable gBN regions. The wBN does not form from gBN by direct or indirect process up to 7 GPa. Around 8.5 GPa, wBN is formed marginally from gBN depending on the starting material. Around 13 GPa, gBN transforms to wBN even at room temperature[16-20]. The wBN transforms completely to cBN around 2100°C at pressures high enough to retain the stability of cBN. The wBN can also be obtained by static compression of gBN and a catalyst in presence of shear stresses[21], and the shock compression of gBN[22-33]. The conversion of gBN to cBN under static pressure in presence of various catalysts is well known[34-39]. The synthesis of cBN under pressure, starting with amorphous gBN is also reported[40].

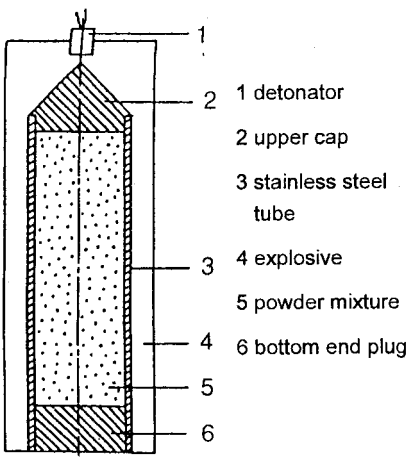

Fig. 2. Schematic of the assembly for a shock loading experiment.

3. PROCESSING OF wBN FOR CUTTING TOOL APPLICATIONS

3.1 Synthesis of wBN

The wBN can be produced from gBN by three distinct methods : (a) the static compression of gBN at very high pressures, (b) static compression of gBN and a catalyst in presence of shear stresses and (c) the shock compression of gBN. The wBN is produced in large quantities by shock compression of gBN. For shock compression, the gBN powder is mixed with a metallic powder (Fe, Cu, Al etc.) and the mixture is contained in a stainless steel ampoule. The metallic powders are used to remove the heat generated during the shock

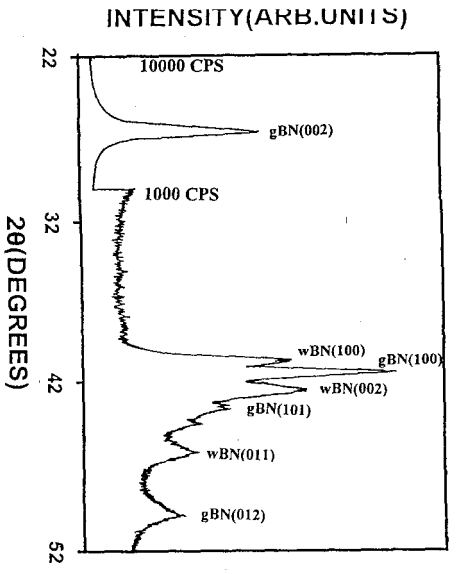

Fig. 3. Typical x-ray diffractogram of the shock loaded sample.

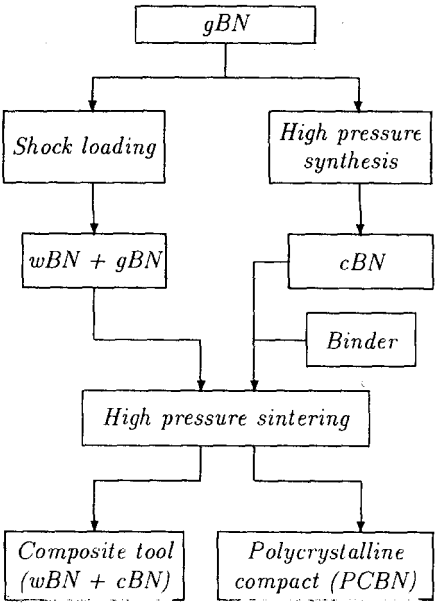

Fig. 4. Flow diagram for the fabrication of wBN → cBN composite. The process for the fabrication of PCBN compact is also shown.

treatment. The shock waves are generated by an explosive charge surrounding the sample (Fig. 2). The fraction of wBN obtained after the shock compression depends on the crystalline state of the starting material, being higher for better crystallized material[24-30]. The rise in temperature during shock compression may lead to a partial wBN → cBN transformation. Thus, the shock-recovered specimen may contain residual gBN phase (Fig.3). The gBN and wBN after shock compression, have a highly defective structure. The high concentration of the defects facilitates the diffusion process in the wBN → cBN transformation during sintering[41]. The wBN transforms to gBN at elevated temperatures and the kinetics study of wBN → gBN transformation in vacuum showed that a complete conversion to the gBN takes place at 1350^0 C in about 30 minutes[42].

3.2 Sintering of wBN powder

The flow diagram for the fabrication of wBN based polycrystalline boron nitride compacts is shown in Fig.4. The wBN powder obtained by shock treatment of gBN is sintered at high pressures and high temperatures to obtain the polycrystalline compacts. The sintering of wBN powder at high pressures are conducted using a Toroid[43,44] type apparatus. The Toroid type-high pressure chamber is shown in Fig.5. It comprises of two identical co-axially placed dies (made of tungsten carbide) one against the other. The dies have a lens like portion in the centre and concentric grooves on their working surfaces. The powder sample to be pressed is placed in the space between the central portions of the dies surrounded by a solid pressure-transmitting medium. The Toroid apparatus is capable of generating pressures

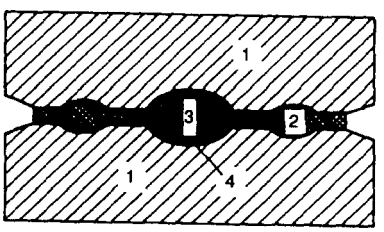

Fig. 5. Schematic of the Toroid-type high pressure-high temperature apparatus (Ref. 27). 1 - WC dies, 2 - pyrophyllite gasket, 3 - sample volume, 4 - graphite heater.

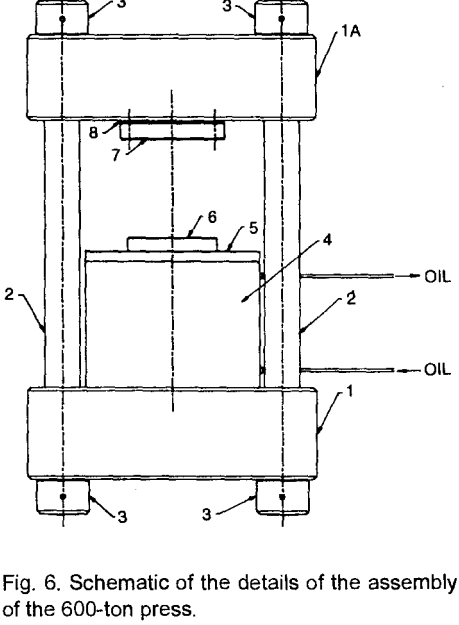

Fig. 6. Schematic of the details of the assembly of the 600-ton press.
1,1A - platens, 2 - tie rods, 3 - tie-rod clamp nuts, 4 - ram cylinder, 5 - cover plate, 6 - ram piston, 7 - top plate and 8 - insulator.

up to 10 GPa at 2300°C with a working volume of ~0.5 cc. The Toroid type apparatus is economical in synthesizing compacts of 3-8 mm diameter and 5 mm long, which can be readily used as cutting tools.

The samples are pressurized by loading the assembly in the 600-ton press [45] (Fig.6). The brief specifications of the press are as follows: (1) tonnage- 640 metric ton, (2) ram diameter-340 mm, (3) stroke of the ram- 100 mm. (4) daylight- 150 mm, (5) operating hydraulic-ram pressure- 700 $kgcm^{-2}$, (6) deflection of platen at full load- 0.06mm, (7) material used- En 24 steel (heat treated and tempered to HRC 42), the yield strength - 150 $kg\ mm^{2}$ and the ultimate tensile strength ~ 180 $kg\ mm^{2}$, (8) variable speed hydraulic pump, (9) factor of safety - 3 and (10) overall dimensions- 820 mm x 680 mm x 1320 mm (height). The samples are heated by using a low voltage - high current transformer (10 KVA, 5V - 2000 A and 10 V - 1000 A).

For the production of the composite compacts, the wBN powder is loaded in a graphite tube (heater) and is assembled in a gasket made of pyrophyllite. The sample is heated by passing high current through the graphite heater. The pressure calibration of the high-pressure assembly were done using the resistance discontinuities at Bi I-II (2.54 GPa), Ba (5.8 GPa) and Bi III-V (7.7 GPa) phase transitions. The power - temperature calibrations are done by measuring the temperature inside the high-pressure cell using a Pt - Pt 10% Rh thermocouple.

The sintering experiments were conducted in the pressure range 5.5 to 7.7 GPa and temperature range 1500 to 1800°C for 30 to 180 s. During an experiment, load was applied corresponding to the desired pressure and the required power was fed to the system. After the sintering time, the power was reduced to zero and then the load was released. The pressure-temperature-time conditions were varied to obtain the wBN - cBN composites with different volume fraction of cBN phase. The sintered compacts can be obtained in various sizes and shapes. The phase composition of the sintered compacts were determined by x-ray diffraction. The extent of wBN → cBN transformation is estimated from the observed angular separation and relative intensities of the composite cBN (111) / wBN (002) and wBN (100) peaks[16].

During pressurization, the wBN particles undergo intense communition due to the action of high static pressures[46-48]. The intensity of communition increases with the increase in starting particle size. The isothermal holding at the sintering temperature at a particular pressure shows that comminution also takes place during sintering. Increase in the isothermal holding duration brings about recrystallization, which leads to the wBN → cBN transformation. The cBN formation in wBN is determined by the combined action of the hot plastic deformation and dynamic relaxation process via fragmentation, polygonization, primary and collective recrystallization[49-51].

Fig. 7. Microstructure of a composite. The cBN grains dispersed in the wBN matrix are seen.

During synthesis, after the release of pressure, a certain fraction of wBN instantaneously transforms to gBN. Therefore, the final sintered compact is a dense body having a composite structure of wBN and cBN with finely dispersed gBN phase (2 - 7 vol. %)[52]. The microstructure of two-phase wBN-cBN composite structure is shown in Fig. 7. The dispersion of cBN grains in the wBN matrix can be seen.

A comparison of the various steps involved in the production of the wBN-cBN composite and PCBN tools (Fig. 4) shows that the cost of the PCBN tools will be higher than those of the composite. This is because, the production of PCBN tools requires cBN powder as the starting material, which itself has to be synthesized at high pressures and temperatures.

4. PROPERTIES OF wBN - cBN COMPOSITE

The mechanical properties of the wBN - cBN composite are dependent on the volume fraction of the cBN phase present in it. Various studies[53-59] on hardness, compressive stress, maximum internal stress, fracture energy and tool wear resistance have shown that the composite with 45 to 55 vol.% cBN has the optimum properties. The hardness of the composites varies from 30 to 70 GPa depending on the volume fraction of cBN present in them. The hot hardness of the optimum composite varies from 70 GPa at room temperature to 20 GPa at 1400 K. The indentation fracture toughness[60] values of the compacts are in the range 13-16.5 MPa $\sqrt{m}$.

4.1 Fracture Toughness of the composite

The high toughness of the wBN cBN composite can be explained in terms of (a) the fine grained structure of the composite, (b) the macro- and micro-stresses which are set up due to the differences in Youngs moduli, volume compression moduli, coefficient of thermal expansion, the anisotropy in elastic properties of the wBN lattice and the difference in the specific volumes of cBN and wBN phases, and (c) the transformation toughening due to the wBN $\rightarrow$ gBN transformation. Super hard materials, in general, follow the classic Griffith-type fracture with failure initiating from the preexisting flaws in the microstructure. In fine grained material, fracture process is controlled by the additional energy being expended in the stage of formation and subcritical crack growth stage and therefore, the work done during crack formation and growth is negligible. Because of this, fine grained superhard materials exhibit higher fracture toughness than the coarse grained ones. On the application of external load, micro cracks initiated by the residual stresses promote stress relaxation at the tip of the crack thereby imparting high fracture toughness in this material. The additional toughening mechanism in the wBN-cBN composite is similar to the transformation toughening mechanism operating in metastable zirconia ceramics[61,62]. *The graphitization that occurs during the release of pressure after* sintering results in an increase of specific volume which sets up compressive stresses around the transformed gBN particles.This leads to rounding of the propagating crack tips and micro-crack formation which impede crack propagation[53]. The formation of micro - cracks is also assisted by the highly anistropic fracture of the gBN due to easy cleavage perpendicular to c-axis.

Table I. Properties of some hard materials (*Ref:13, 63, 64; †Ref:65; ‡Ref:66)

Property	K_{20}†	PCD-10†	Amborite†	DBC-50‡	wBN-cBN composite*
Density, (gcc^{-1})	14.70	4.12	3.42	-	3.39-3.44
Young's Modulus (GPa)	620	776	680	587	760
Compressive strength (GPa)	4.5	7.6	2.73	-	3.4
Bending strength (GPa)	2.07	1.26	0.57	-	1.2
Knoop hardness (GPa)	13	50	32	28	30-70
Fracture toughness (MPa $\sqrt{m}$)	10.8	7.3	6.3	3.7	13-16
Coefficient of thermal expansion (10^{-6} K^{-1})	5.4	4.2	4.9	4.7	2.7 3.7
Thermal conductivity ($Wm^{-1}K^{-1}$)	100	560	100	44	40-50

A comparison of the various properties of wBN - cBN composite with tungsten carbide (K_{20}), Poly Crystalline Diamond (PCD), amborite (amber boron nitride particles with metallic binder), DBC50 (finer cBN particles dispersed in TiC with aluminium diboride and nitride) are given in the Table I. It can be seen that the fracture toughness of composite is very high, as compared to those of diamond and cBN based materials and similar to that of WC-10Co cemented carbide.

5. PERFORMANCE OF COMPOSITE TOOLS

The main application of the composite tool is in the machining of hardened steels, cast irons, hard alloys and other difficult-to-cut materials. The distinguishing feature of the composite tool is its capacity to operate under impact loads during machining. The economic use of polycrystalline boron nitride tool in machining hard ferrous alloys (over HRC 45) is based on the principle of self - induced hot machining. In conventional tool materials, it is a standard practice to employ positive rake angle and low cutting speeds to reduce the cutting forces and temperatures. In contrast, superhard material tools require negative rake angle and relatively higher cutting speeds. The negative rake angle together with the higher cutting speed, generates heat which continuously softens the work piece in the small volume of the cutting zone. The temperatures generated at the shear zone are high enough for the cutting edge and the chips to become red hot. The softening of the work-material, due to heat generated by the friction and intense shear strain, makes it possible to machine steels harder than HRC 60 continuously for longer periods. The heat generated is taken away by the chip or the tool which has a high thermal conductivity (40-50 $Wm^{-1}K^{-1}$). The work piece therefore remains cool and its hardness is not affected.

The wBN-cBN compacts obtained by high pressure-high temperature sintering were metallized and brazed on to steel holders. The tool tips were ground to the required geometry using diamond wheels. The tool geometry used in the present investigations is as follows : clearance angle 12°, rake angle - -11°, end relief angle 15°, plan approach angle 45° and nose radius 0-3 to 0.4 mm. The work materials used for the machining tests were hardened tool steel (HRC 60-63), hardened alloy steel (HRC 40-43), high

Table II. Performance of the wBN - cBN composite tools

Work material	Tool material	Machining conditions	Tool life (min) /V_B (mm)	Finish/time Ra (μm)/min
Tool steel HRC 60 - 63	wBN-cBN composite	s - 80m/min f - 0.075mm/rev doc - 0.2mm continuous	138/0.4	0.39(30)
		discontinuous	135/0.28	
EN24 HRC 40-43	wBN-cBN composite	s - 80m/min f - 0.075mm/rev doc - 0.2mm	108/0.38	0.85 (15)
	Carbide (P_{30}) coolant used	s - 80m/min f - 0.075mm/rev doc - 0.2mm	48/blunt	2.61 (30)
Cast iron BHN 120-160	wBN-cBN composite	s - 340m/min f - 0.1mm/rev doc - 0.5mm	-	0.45 (20)
	Carbide (K_{20})	s - 80m/min f - 0.1mm/rev doc - 0.5mm	-	2.65 (15)
Ti-6Al-4V HV 310 (water based coolant used)	wBN-cBN composite	s - 75m/min f - 0.1 mm/rev doc - 0.5 mm	80 (0.28)	1.08 (80)
	Carbide (K_{20})	s - 75m.min f - 0.1 mm/rev doc - 0.5 mm	12	1.52 (12)

nickel cast iron (BHN 120-160), Ti-6Al-4V alloy (HV 310) and Al- SiC_p MMCs. The turning tests were conducted on 60 mm diameter and 300mm long steel and cast iron rods. The machining conditions, tool life, surface finish obtained while machining hardened steels, cast iron and titanium alloy are given in Table II. The tool life was determined by measuring the flank wear width of the tool V_B. The limiting value was set as 0.4 mm in case of ferrous materials. The tests were also carried out under interrupted cutting conditions by providing a 5 mm wide axial slot in the work piece. The machining tests were also carried out using P_{30} grade cemented carbide for En24 steel and K_{20} grade cemented carbide tools for cast iron and titanium alloy.

Various types of wear can take place in a turning tool. At the cutting edge, wear is normally observed on the rake face and flank face. Wear on the rake is characterized by the formation of the crater due to the flow of the chip along the face. Wear on the flank is caused by the abrasion of the freshly cut surface. At low cutting speeds, the flank wear rate is faster than the crater wear. The abrasion resistance of a tool is often related to its hardness. The abrasion wear is minimized if the hot hardness of the tool material is greater than that of the hard particles present in the work material. At higher cutting

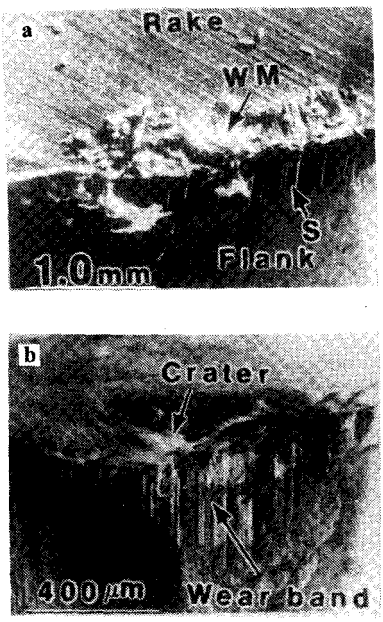

Fig. 8. Composite tool after machining a) hardened steel (HRC 61-63) for a) 2 min. and b) 20 min.at 80m/min.cutting speed, 0.075mm/rev feed and 0.2mm depth of cut.

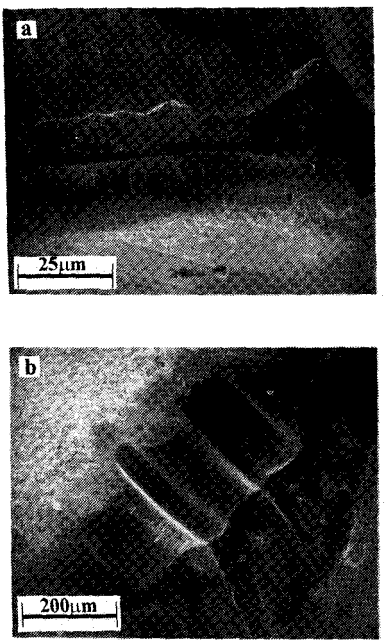

Fig. 9. Composite tool after machining high nickel cast iron (BHN 120-150) for a) 2 min. showing rounding off of the cutting edge and b) 20 min. showing grooves both on the rake and the flank. The cutting conditions are speed - 340m/min., feed - 0.1mm/rev and depth of cut - 0.5mm.

speeds, the crater wear takes place mainly due to the chemical instability of the tool material-work material combination at elevated temperatures.

5. Hardened steel and cast iron

Our earlier studies[11] on the wear characteristics of the composite tools while machining ferrous alloys have shown that the wear on the tool occurs in various stages. Initially, after ~ 2min.of machining, sticking of the particles from the work piece to the cutting edge is seen (Fig 8a). Once proper contact between the tool and the work piece is established, a wear band is formed on the flank (Fig.8b). On continued cutting, the crater which develops on the rake deepens and increases the rake angle in the positive direction This weakens the tool and leads to further microspalling. Under favorable conditions, the wear bands disappear during the microspalling and the wear cycle is repeated.

In cast iron machining, initially rounding off of the cutting edge takes place (Fig. 9a). The wear on the tool is due to the formation of grooves close to the major cutting edge. In steel machining, there is continuous chip formation and the maximum temperature is generated on the rake face away from the cutting edge. Whereas, in cast iron machining, the chip is segmented and the highest temperature is generated closer to the cutting edge[67-69]. In addition, the temperature on the flank face may be equal to or even more than the temperature on the rake face[70-72]. This unfavorable temperature distribution and the high abrasiveness of cast iron leads to groove formation on both rake and flank face (Fig.9b).

In interrupted cutting, the wear on the tool takes place by the formation of cracks, which are generated due to thermal and mechanical fatigue. Thermal cracks are formed due to

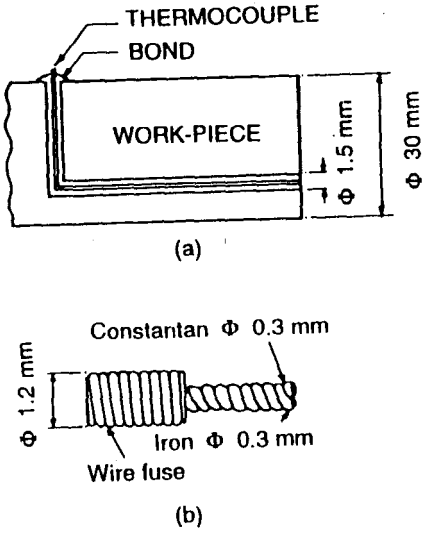

Fig. 10. a) Arrangement of the thermocouple wires in the work piece. b) Twisted insulated thermocouple wires wound with fuse wire for stable thermal contact (Ref.81).

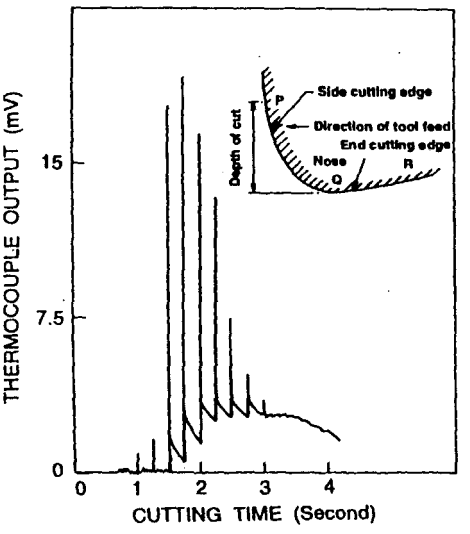

Fig. 11. Typical record of the temperature at the tool edge. The spikes result when the cutting edge makes contact with the thermocouple wires.

the large temperature gradient and temperature fluctuation during cutting and non-cutting periods. These cracks form either on the rake or on the flank or on both in a direction perpendicular to the cutting edge. Such cracks are not observed in the wBN-cBN composite tools. The necessary property of high thermal shock resistance may be attributed to the high thermal conductivity and fracture toughness of the composite tools. The cracks on the flank parallel to the cutting edge are associated with the mechanical fatigue[72-73].

5.2 Titanium alloy

The machining of titanium alloys is difficult due to its high chemical affinity and the generation of high temperatures[74-80] locally because of its poor thermal conductivity (8 W $m^{-1}K^{-1}$). PCD and PCBN tools have been used for machining titanium and the former are reported to perform better[79]. The temperatures generated at the cutting edge while machining[81-82] was estimated as follows: two insulated thermocouple wires were introduced in the work piece and these were cut together with the work piece forming the junction, and the output was recorded. The location of the thermocouple on the work piece and a typical record of the temperature are shown in Figures 10 and 11. While machining, a number of contacts are made between the thermocouple and the tool starting from P (point on the side cutting edge) to R (point on the end cutting edge). A temperature spike is recorded every time the cutting edge contacts the thermocouple. The spike height increases with the increase in the number of contacts and decreases after passing through the tool nose (point Q). The estimated temperature is around 1200K. The details are given elsewhere [81]. The tool shows the formation of an adherent layer due to the chemical reaction between titanium and, the boron and nitrogen present in the tool along the cutting edge (Fig.12a). The mechanism of formation of this layer is similar to that reported on PCD tools[80] where the interdiffusion of titanium and carbon resulted in the formation of a titanium carbide layer on the rake. The reaction layer grows with cutting time until a stress level is reached which will cause fracture. The strong adherence of the

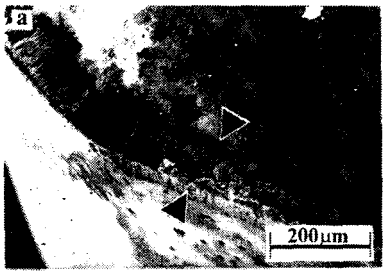

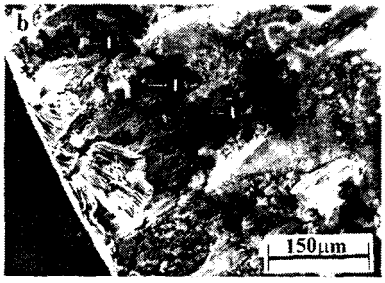

Fig. 12. Composite tool after machining titanium alloy (HV 310) after a) 10 min. showing the layer formation and b) 50 min. showing the detachment of the hard particles leading to uneven crater wear at 75 m/min. (speed), 0.1 mm/rev (feed) and 0.5 mm (doc).

Table III. Details of the MMCs

Composition	SiC particle size (μm)	Diameter,mm (hardness BHN)
Al-30%SiC (as cast)	14	70 (90)
Al-25%SiC (extruded) (RRL, Trivandrum, India)	32	90 (130)
Al-7.5Si-3Mg-15%SiC (extruded, hydro-Aluminium, Norway)	23	100 (220)

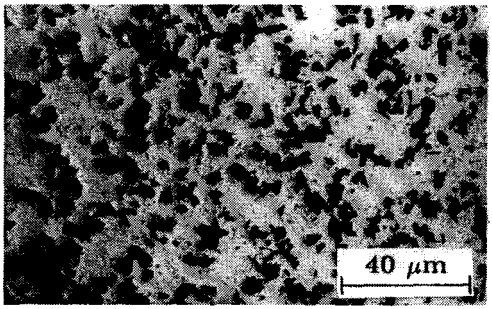

Fig. 13. Typical microstructure of the Al-SiC_p MMC. The dark spots are SiC particles with an average size of 14 m.

layer often causes detachment of hard particles from the tool and leads to uneven cratering (Fig. 12b). The high hot hardness of the wBN-cBN composite prevents deep cratering and enables the tool to continue machining without immediate failure. The attrition wear on the flank leads to the weakening of the cuting edge and failure of the tool will occur. The high fracture toughness of the wBN-cBN composite plays an important role during this period in delaying the fracture of the tool. The high hot hardness and fracture toughness of the wBN - cBN composite contribute to the success of the tool.

It is clear from the data presented in Table II that the composite tools perform very much better both in terms of life and the surface quality obtained compared to the cemented carbide tools. While machining cast iron, the composite tools can be operated at ~5 times the speed of the carbide tools with better surface finish. In machining titanium alloy, the superiority of the composite tool is clear. In identical machining conditions, the cemented carbide tools failed after about 12 min. whereas, the composite tool did not fail even after 80 min.

5.3 Metal Matrix Composites

Aluminium (base metal) matrix composites (MMCs) are attractive materials for aerospace applications due to the unique combination of their strength and lightness. The MMCs are extremely abrasive and are difficult- to-cut materials. The conventional tool materials (HSS and cemented carbides) fail due to the high hardness of the reinforcements in the

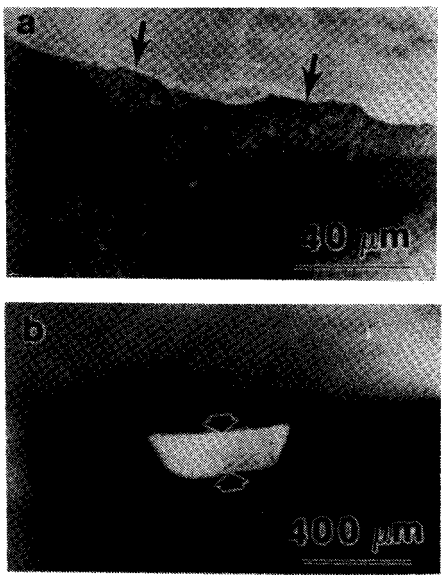

Fig. 14. Composite tool after 3 min. of machining a) before etching showing sticking of the work-material and b) after etching with NaOH solution showing the polished region of the nose, Cutting conditions: speed 175 m/min, feed - 0.1 mm/rev and doc 0.25 mm.

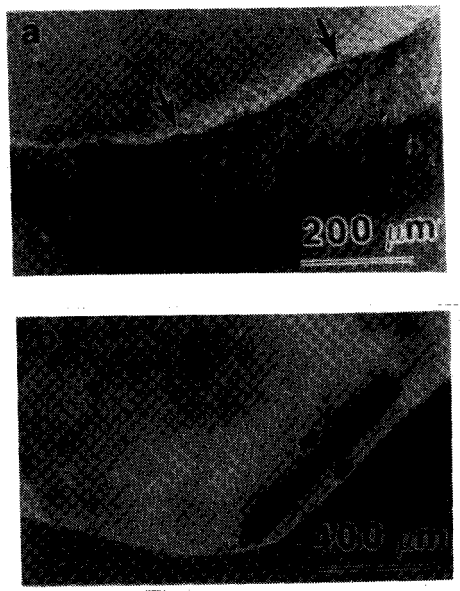

Fig. 15. Composite tool after 8 min. of machining showing a) formation of Built Up Edge (BUE) and flank wear and b) crater after etching. Cutting conditions same as in Fig.14.

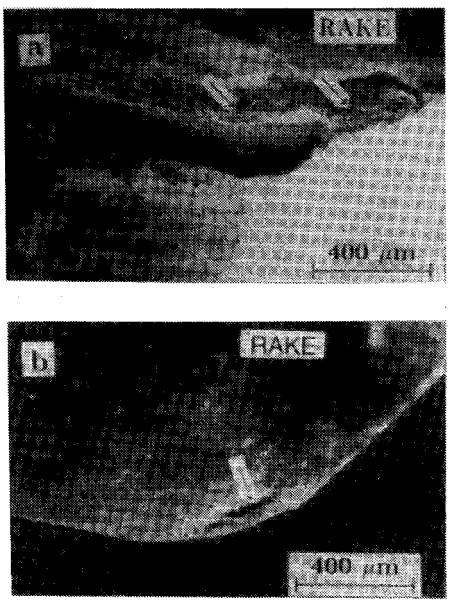

Fig. 16. Composite tool after 8 min. of machining showing formation of crater a) before etching and b) after etching). Cutting conditions same as in Fig.14 except that the doc -1 mm.

MMCs. Various studies have been made on the machining of MMCs[84-91]. PCD tools have been found to be suitable for machining MMCs, but are expensive.

The composition, SiC particle size, hardness and diameter of the work piece are presented in Table III. The typical microstructure of the MMC is shown in Figure 13. The dry machining tests were conducted using single point wBN-cBN composite turning tools.

The SEM and optical photographs of the worn cutting tools are shown in Figs.14-16. Intially (30s of machining), sticking of the work-material on the rake along the cutting edge is observed. On continued machining (3 min), more work-piece material is found to adhere on the rake forming the built-up-edge (BUE) at the nose (Fig. 14a). The formation of the wear band at the nose is observed, whereas the major cutting edge and and flank remained unaffected. On careful examination, it was found that a thin layer of MMC was adhering at the nose region. After removal of this layer (dissolving in strong NaOH solution), it was observed that the tool

nose got polished due to the abrasive action of the SiC particles (Fig.14b). The amount of the material removed from the nose region by the abrasive wear is very small and it is hardly possible to find any change in the cutting tool geometry. No wear was observed on the rake, flank or at the cutting edge. The tool after 8 min. of machining is shown in Fig.15. A comparison of the worn tools (Figs. 14a and 15a) reveals that the profile of the cutting edge has changed. The formation of a thin crater region parallel to the cutting edge, but away from it is seen in Fig. 15b.

The results indicate that the wear on the tool while machining MMC is due to the abrasion between the tool and the work-piece. Various theories[92-94] have been put forward to explain how abrasive wear occurs on cutting tools. It has been shown that the abrasion takes place by microcutting when the hardness of the abrasive particles in the work-material is equal to or greater than that of the tool material. When the hardness of the abrasive particles is less than that of the tool material, as the cutting edge strikes a hard partcle, the kinetic energy transferred from the particle to the tool is proportional to the cube of the particle size and to the square of the cutting speed[85]. Abrasive wear is the accumulated micromechanical damage caused by these impacts.

In the present case, as the tool material is harder than the reinforcement (SiC), the wear may be associated with the micromechanical damage rather than micro cutting. The wear process on the rake and flank faces can be classified as sliding wear. The free particles which are separated from the tool by microcracking and fatigue can act as a polishing compound between the chip, work-piece and the tool (three body wear)[87].

It is observed that the wear takes place, first at the nose region (Fig. 14). With continued machining, sufficient contact zone is formed between the tool and the work-piece and the wear progresses on the flank forming a band parallel to the major cutting edge (Fig. 15). The thickness of the wear band on the nose and the flank increases as the cutting progresses (Fig. 15b). This wear band region has been observed to be highly polished (Fig. 14b) indicating that, the material removal from the tool is in a very fine scale. This also indicates that the bonding between the grains of the hard particles in the tool is very strong and resists the severe grinding conditions expected in three-body-wear.

The high strain rate generated at high cutting speeds (175 m/min) and the friction between SiC particulate and the tool raise the cutting temperatures much above those generated in the machining of conventional aluminium alloys. It is possible that the aluminium matrix softens to a considerable extent or even melts in a very small volume at the contact zone between the tool and the work-material. As a result, it adheres to the tool forming BUE (Figs. 14a and 15a) and prevents the direct contact between the tool and the work-material. The sliding action of the chip with the rake of the tool gets shifted away from the cutting edge and results in the formation of crater in the form of a parallel band away from the cutting edge. On continued cutting, the BUE grows (Fig. 15a) and causes an increase in the cutting force. The material at the BUE gets work hardened due to the repeated deformation and breaks away from the tool. The adhesion between the BUE and the tool is so strong that, during this breaking process, some material is plucked from the tool. When the depth of cut was increased to 1mm, the BUE formed on the rake was found to break away plucking with it some tool material resulting in a deep crater (Fig. 16). The surface finish on the MMCs obtained in comparison with those obtained using WC based tools are presented in Table IV. It is clear that the performance of the wBN-cBN composite tools is superior to that of WC based tools. The composite tools can be operated at 10 times the speed of the WC based tools with better surface finish.

Table IV. Surface finish on MMCs

Material	Tool cutting conditions	Time (minutes)	R_a	R_z (μm)	R_t
Al-25SiC (32μm)	Tungsten Carbide s - 20m/min f - 0.1 mm/rev doc - 0.25 mm	7	1.37	7.31	10.57
	wBN-cBN Composite s - 175 m/min f - 0.1 mm/rev doc - 0.25 mm	3	1.42	3.17	11.39
		6	1.07	5.70	8.22
Al-7.5Si-3Mg-15SiC (23μm)	Tungsten Carbide s - 20m/min f - 0.1mm/rev doc - 0.25mm	9	2.02	12.68	20.07
	doc - 0.50 mm	6	1.51	6.20	9.44
	doc - 1.00 mm	6	0.82	4.40	6.20
	wBN - cBN Composite s - 175 m/min f - 0.1 mm/rev doc - 0.25 mm	1.5	0.87	6.12	5.69
		4.5	0.48	3.16	5.54
		9	0.24	1.67	2.80
	doc - 1.0 mm	6	0.63	4.15	5.92

6. CONCLUSIONS

The wBN-cBN composite has an excellent combination of properties (hardness, fracture toughness and inertness), and it has been demonstrated that these tools can be used to machine hardened steels, cast irons, titanium alloy and Al-SiC_p MMCs economically. These tools can be used for hard-machining of steels in both continuous and intermittent cutting conditions, and hence avoid the grinding operation. The composite tools can machine cast iron at ~5 times faster than the cemented carbide tools and the life of the tool while machining titanium alloy is ~7 times that of the carbide tools. In most of the cases no coolant is necessary. The temperatures generated while machining titanium alloy is 1200 K and the wear of the tool can be associated with the chemical interaction between the tool and the work piece. The wear while machining the MMC can be modelled as a three body wear. The high fracture toughness of the composite allows them to be used on non-rigid machines. The wBN-cBN composite fills the gap between carbide based and the expensive PCBN tools for machining hard ferrous materials.

ACKNOWLEDGEMENTS

This work was carried out with the support and guidance of A.K.Singh and active participation of S.K.Bhaumik. I thank B.N.Acharya, M/s IDL, Hyderabad for the shock loading experiments. L.Rangaraj, Y. Ramachandra and Jayaprakash have assisted in the

preparation of the specimens for the shock loading, and conducting the sintering experiments. Thanks are due to B.C.Pai of RRL, Thiruvananthapuram for providing the MMC samples. The help received from V.Narayanaswamy, T.Irudayaraj, P.M.Jaman and C.Swamy in conducting the machining trials, Mr M.A.Venkataswamy for scanning electron microscopy and S.Usha Devi for x-ray analysis is gratefully acknowledged.

REFERENCES

1. Wentorf, R .H., J. Chem. Phys., 1957, **26**, 956
2. Bovenkerk, H. P., Bundy, F. P., Hall. H. T., Strong, H. M., and Wentorf, R. H., Nature, 1959, **184**, 1094
3. Wentorf, R. H., J. Chem. Phys., 1961, **34**, 809
4. Materials Sci. and Engg. for the 1990s, National Research Council 1990, 25
5. Vel, L., Demazeau, G., and Etourneau, J., Mat.Sci. and Engg., 1991, **B10**, 149
6. Tomlinson, P. N., and Wedlake, R. J., Speciality steels and hard materials, 1983, 173
7. Modi, H. J., Workshop on high pressure techniques in metal forming and materials synthesis, 1985
8. Bhaumik, S. K., Divakar, C., and Singh, A. K., Metals Materials and Processes, 1993, **5**, 199
9. Trefilov, V.I., Frantsevich, I.N., etal, Sint.Almazy (Russian), 1974, **4**, 24
10. Divakar, C., Bhaumik, S.K., and Singh, A.K., Metals Materials and Processes, 1994, **6**, 51
11. Bhaumik, S.K., Divakar, C., Singh, A.K., and Bochko, A.V., Metals Materials and Processes, 1994, **6**, 39
12. Divakar, C., Bhaumik, S. K., and Singh, A. K., Advances in High Pressure Science and Technology, 1995, 282
13. Kurdyumov, A. V., Pilyankevich, A. N., and Frantsevich, I. N., Poroshkovaya Metallurgiya, 1973, **10**, 57
14. Kurdyumov, A. V., and Pilyankevich, A. N., Phase Transformations in Carbon and *Boron nitride (Russian), 1979*
15. Bundy, F. P., and Wentorf, R. H., J. Chem. Phys., 1963, **38**, 1144
16. Corrigan, F. R., and Bundy, F. P., J. Chem. Phys., 1975, **63**, 3812
17. Wakatsuki, M., Ichinose, K., Aoki, T., Mat. Res. Bull., 1972, **7**, 999
18. Ichinose, K., Wakatsuki, M., Aoki,T., and Maeda,Y., Proc.4 AIRAPT Conf.,1975, 441
19. Wakatsuki, M., Ichinose, K., Proc.4 AIRAPT Conf., 1975, 436
20. Wakatsuki, M., Takano, K. J., and Fujita, G., Physica, 1986, **139 and 140B,** 256
21. Vereschagin, L. F., Zubova, E. V., Burenkova, L. N., and Revin, N. I., Dokl. Akad. Nauk SSSR, 1968, **178**, 72

22. Altshuler, L. V., Pavlovskii, M. N., and Drakin, V. P., Zh. Eksperim. i .Teor. Fiz, 1967, **52**, 400
23. Adadurov, G. A., Aliev, Z. G., Atovmyan, L. O., Bavina, T. V., Borodko, Yu. G., Breusov, O. N., Dremin, A. N., Muranevich, A. Kh., and Pershin, S. V., Dokl. Acad. Nauk SSSR, 1967, 172, 1066
24. Decarli, P. S., Bull. Am. Phys. Soc., 1967, **12**, 1127
25. Coleburn, N. L., and Forbes, J. W., J. Chem. Phys., 1968, **48**, 555
26. Johnson, Q., and Mitchell, A. C. , Phys. Rev. Lett., 1972, **29,** 1369
27. Soma, T., Sawaoka, A., and Saito, S., Mat. Res. Bull., 1974, **9**, 755
28. Soma, T., Sawaoka, A., and Saito, S., Proc.4 AIRAPT Conf., 1975, 446
29. Wakatsuki, M., and Ichinose, K., Proc.4 AIRAPT Conf., 1975, 441
30. Saito, S., and Sawaoka, A., High Pressure Sci. and Tech., 1979, **1,** 986
31. Saito, S., and Sawaoka, A., High Pressure Sci. and Tech., 1980, **1,** 541
32. Araki, M., and Kuroyama, K., Physica, 1986, **139 & 140B**, 819
33. Sekine, T., J. Mat.Sci.Lett., 1989, **8,** 872
34. Devries, R. S., and Fleischer, J. F., Mat. Res. Bull., 1969, **4,** 433
35. Susa, K., Kobayashi, T., and Taniguchi, S., Mat. Res. Bull., 1974, **9**, 1443
36. Endo, T., Fukunaga, O., and Iwata, M., J. Mat. Sci., 1979, **14**, 1375
37. Kobayashi, T., J. Chem. Phys., 1979, **70**, 5898
38. Kobayashi, T., Mat. Res. Bull., 1979, **14**, 1541
39. Endo, T., Fukunaga, O., and Iwata, M., J. Mat. Sci., 1979, **14**, 1676
40. Sumiya, H., Iseki, T., and Onodera, A., Mat. Res. Bull., 1983, **18**, 1203
41. Kurdyumov, A. V., Poroshkovaya Metallurgiya, 1975, **12,** 69
42. Kurdyumov, A. V., Ostrovskaya, N. F., Pilyankevich, A. N., Balan, T. R., and Bochko, A. V., Poroshkovaya Metallurgiya, 1976, **1**, 64
43. Vereschagin, L. F., Galaktionov, A., Semerchan, A. A., and Slesarev, V. N., Dokl. Akad. Nauk SSSR, 1960, **132**, 1059
44. Vereschagin, L. F., Khvostantev, L. G., and Novikov, A. P., High Temp.-High Press., 1977, **9**, 637
45. Saravana, B. V., Gopalakrishna, V. D., Venkatachalam, K., Jaman, P. M., Divakar, C., and Singh, A. K., Advances in High Pressure Sci. and Tech., 1995, 401
46. Dzhamarov, S. S., Poroshkovaya Metallurgiya, 1982, **6**, 238
47. Dzhamarov, S. S., and Schcherban, N. I., Poroshkovaya Metallurgiya, 1983, **2**, 32
48. Kovalchenko, M. S., and Dzhamarov, S. S., Poroshkovaya Metallurgiya, 1984, **2**, 31
49. Frantsevich, I. N., and Balan, T. R., Dokl. Akad. Nauk SSSR, 1984, **218**, 591
50. Kurdyumov, A. V., Poroshkovaya Metallurgiya, 1976, **1**, 64
51. Kurdyumov, A. V., Poroshkovaya Metallurgiya, 1986, **4**, 96

52. Kurdyumov, A. V., Oleinik, G. S., Pilyankevich, A. N., Balan, T. R., Bochko, A. V., and Dzhamarov, S. S., Poroshkovaya Metallurgiya, 1976, **10**, 47

53. Bochko, A. V., Grigoriev, O. N., Dzhamarov, S. S., Karyuk, G. G., Milman, Yu. V., and Trefilov, V. I., Poroshkovaya Metallurgiya, 1977, **6**, 4

54. Bochko, A. V., Grigoriev, O. N., Dzhamarov, S. S., Karyuk, G. G., Kurdyumov, A.V., Oleinik, G.S ., Pilyankevich, A. N., Trefilov, V. I., Frantsevich, I. N., and Shatokhin, A. N., Poroshkovaya Metallurgiya, 1979, **10**, 61

55. Bochko, A. V., Grigoriev, O. N., Dzhamarov, S. S., Pilyankevich, A. N., Trefilov, V. I., Karyuk, G. G., Frantsevich, I. N., and Shatokhin, A. N., Poroshkovaya Metallurgiya, 1980, **5**, 96

56. Grigoriev, O. N., Dzhamarov, S. S., Trefilov, V. I., and Shatokhin, A. N., Poroshkovaya Metallurgiya, 1981, **1**, 53

57. Grigoriev, O. N., Dzhamarov, S. S., Trefilov, V. I., and Shatokhin, A. N., Diamond Superhard Material, 1981, **7**, 4

58. Bochko, A. V., Grigoriev, O. N., Svyazkina, T. M., and Shatokhin, A. N., Poroshkovaya Metallurgiya, 1986, **4**, 87

59. Trefilov, V. I., Milman, Yu. V., and Grigoriev, O. N., Prog. Crystal Growth and Charact., 1988, **16**, 225

60. Evans, A. G., and Charles, E. A., J. Am. Ceram. Soc., 1977, **59**, 371

61. Pilyankevich, A. N., and Claussen, N., Mat. Res. Bull., 1978, **13**, 413

62. Claussen, N., J. Am. Ceram. Soc., 1978, **61**, 85

63. Karyuk, G. G., Bochko, A. V., Yarosh, V. V., Dzhamarov, S. S., Volkogon, V. M., and Aronovich, A. O., Proc. XI AIRAPT Conf., 1989, **vol 2**, 128

64. Primachuk, V. L., Bochko, A. V., and Avetisyan, A. O., Poroshkovaya Metallurgiya, 1983, **8**, 80

65. Bossom, P. K., IDR., 1990, **50**, 228

66. Hooper, R. M., Shakib, J. I., Parry, A., and Brookes, C. A., IDR., 1989, **49**, 170

67. Trent, E. M., New Tool Materials and Cutting Techniques, Engg,Digest Tech. Conf., 1977

68. Trent, E. M., Metal Cutting, 1977

69. Shaw, M. C., Metal Cutting Principles, 1984

70. Dearnley, P.A., Wear. 1985, **101**, 33

71. Brandt, G. A., Mikas, M., Senesan, Z., and Hogmark, S., Surface Engg., 1987, **3**, 211

72. Flomn, D. G., Reed, W. R. Jr., Hibbs, L. E.Jr., and Broskea, T. J., Wear, 1991, **147**, 253

73. Mertin, C. W., Science of Hard Materials, 1983, 757

74. Bex, P. A., IDR 1977, **36**, 276

75. Hartung, P. D., and Kramer, B. M., Annals of CIRP., 1982, **31**, 75

76. Milbrandt, A., and Seidenfaden, A., IDR., 1976, **36**, 134

77. Narutaki, N., and Murahoshi, A., Annals of CIRP., 1983, **32**, 65
78. Kahles, J. F., Field, M., Eylon, D., and Froes, F. H., J. Metals, 1985, **37**, 27
79. Dearnley, P. A., and Grearson, .A. N., Mat. Sci. and Tech., 1986, **2**, 47
80. Brookes, C. A, James, R.D., and Nabhani, F., IDR., 1991, **36**, 89
81. Sakuma, K., and Seto, M., Bull. JSME, 1981, **24**, 748
82. Hirao, M., and Sata, T., J. Jap. Soc. Prec. Engg., 1974, **40**, 156
83. Bhaumik, S. K., Divakar, C., and Singh, A. K., Materials and Design, 1995, **16**, 221
84. Chadwick, G. A., and Heath, P. J., Metals and Materials, 1990, **6,** 73
85. Eastman, M., and Lane, C., Cutting Tool Engg., 1993, **45,** 38
86. Jennings, M., IDR., 1993, **1,** 1
87. Weinert, K., and Bierman, D., Machining of Advanced Materials, Proc. Int. Conf. On Machining of Advanced Materials, 1993, NIST Publication **847,** 437
88. Weinert, K., Annals of CIRP., 1993, **42,** 95
89. Yuan, Z. J., Annals of CIRP., 1993, **42,** 107
90. Clark, I. E., IDR. 1994, **54**, 135
91. Masounave, J., Litwin, J., and Hamelin, D., Materials and Design, 1983, **32**, 65
92. Suh, N. P., Wear, 1973, **25**, 111
93. Suh, N. P., Carbide Journal, 1977, **9**, 3
94. Suh, N. P., Wear, 1980, **62**, 1